Microscopic analysis of $\vec{t} + {}^{12}C$ scattering

D. P. Sanderson, J. A. Carr, and K. W. Kemper
Department of Physics, Florida State University, Tallahassee, Florida 32306
(Received 10 June 1985)

Optical model calculations with double-folded microscopic real central and spin-orbit potentials and an imaginary Woods-Saxon potential have been carried out for previously reported $\vec{t} + {}^{12}C$ and ^{58}Ni elastic scattering data. The $\vec{t} + {}^{12}C$ calculations are not able to reproduce the changes in the measured analyzing powers as a function of bombarding energy, whereas they do describe the $\vec{t} + {}^{58}Ni$ data. This analysis suggests that information about the cluster-core $\vec{t} + {}^{12}C$ spin-orbit potential, necessary for cluster structure calculations, cannot be determined without considerably more data. Three-particle-transfer reactions leading to ^{15}N show numerous structures that could appear in the $t + {}^{12}C$ entrance channel. Excitation functions are needed for both the elastic and 4.43 MeV first excited state in ^{12}C if this scattering is to be understood.

Early heavy-ion induced three-particle transfer reactions[1] showed a much larger than expected selectivity in the final state populations, suggesting that triton and ^3He clustering occurred in light nuclei. A cluster potential model, developed by Buck and co-workers,[2] is successful in describing the observed selectivity in terms of alpha and three-particle cluster states in the $15 < A < 20$ mass region. A necessary part of the three-particle cluster-core interaction potential is that arising from the spin-orbit force between the cluster and the core. From an analysis of three-particle cluster transfer reactions in these light nuclei, one arrives at a spin-orbit potential with a depth of between 2 and 4 MeV.[2,3] In contrast, a recently reported analysis of $\vec{t} + {}^{12}C$ analyzing power data showed evidence for spin-orbit potential strengths that are more than five times deeper.[4] Because of the importance of knowledge of the cluster-core spin-orbit potential in understanding triton and ^3He clustering in light nuclei, this conflict must be understood.

One difficulty with this recent analysis[4] of $\vec{t} + {}^{12}C$ is that the spin-orbit potential strength decreased from 16.4 to 8.7 MeV with only a 2 MeV change in the incident triton energy. This change was accompanied by a simultaneous increase in the surface absorption from 9.7 to 18.3 MeV. The rapid variation with energy of the absorption and spin-orbit parameters suggests that the optical model fits might include effects due to resonances in the ^{15}N compound nucleus. It has been proposed[5] that the rapid change in the energy dependence of the spin-orbit potential arises from the excitation of giant multipole resonances in ^{15}N, but the factor of 2 change in the imaginary potential was not considered in this analysis. The $^{12}C(^7Li,\alpha)$ three-particle transfer reaction, which can populate states in ^{15}N that would also be reached from the $t + {}^{12}C$ channel, gives an indication that there may be narrow resonances in addition to the giant resonance already postulated.[5] Figure 1 shows a spectrum from this reaction taken at 48 MeV,[6] with the two arrows indicating the triton bombarding energies of 9 and 11 MeV. Prominent structures are observed in ^{15}N around these energies. For the $(^7Li,\alpha)$ reaction, the angular momentum mismatch at 22 MeV excitation energy in ^{15}N is about $7\hbar$. The critical angular momentum ($T_l = \frac{1}{2}$) for the triton elastic scattering is also about $7\hbar$, suggesting that the states in ^{15}N populated by this transfer reaction can couple strongly to the $t + {}^{12}C$ elastic scattering channel.

To investigate the possible influence of entrance channel effects on the elastic scattering, we have examined the triton elastic scattering data from two points of view. We first examined whether the data admit a description by any energy independent potential. We then undertook a double-folding model analysis that incorporates a microscopic model of the spin-orbit optical potential. The corresponding reduction in the number of free parameters reduces (but cannot eliminate) the likelihood that resonance effects in the analyzing powers can be mocked up by a change in the strength or geometry of the spin-orbit potential.

Some insight into the scattering can be gained by direct examination of the energy dependence of the data. Figure 2 displays the $\vec{t} + {}^{12}C$ data at four energies: 9, 11, 15, and 17 MeV.[4,7] The cross sections show a definite pattern out to approximately 60°. A large dip, starting at approximately 40° for 9 MeV, slowly moves to smaller angles with increasing energy. The analyzing powers also show similar structure at the forward angles, with an oscillation moving slowly inward with energy. However, it is also evident that the magnitudes of these structures vary unpredictably with energy, suggesting that a simple description of the data may not be possible. At angles greater than 60° the angular distributions of cross section and analyzing power diverge with energy. All four show radical differences at the more backward angles, another indication that coupled channels effects could be important here. The next step was to determine whether any reported parameter set, either in Ref. 4 or Ref. 7, can describe the scattering at more than one energy. To that end, calculations were performed for the data at each energy with all reported parameter sets for $\vec{t} + {}^{12}C$. For example, Fig. 3 shows the 9 MeV data with a calculation us-

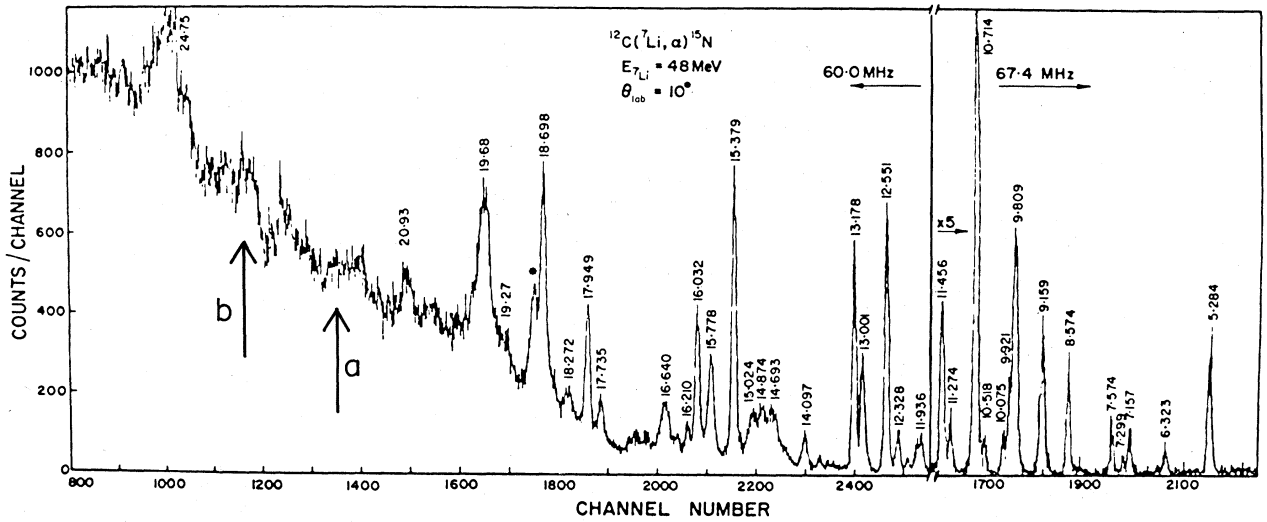

FIG. 1. $^{12}C(^7Li,\alpha)$ spectrum at a laboratory angle of 10° and a ^7Li energy of 48 MeV (from Ref. 6). The arrows denote the energies in ^{15}N excited by 9 (a) and 11 (b) MeV triton elastic scattering from ^{12}C.

ing the Woods-Saxon potential obtained from the analysis of cross section and analyzing power data taken at 17 MeV.[7] Only data out to 90° c.m. was used to produce the 17 MeV fit. As can be seen, the description of the data was poor. We carried out extensive parameter searches and no Woods-Saxon (WS) shaped optical model potential could be found which would describe the data at any two energies simultaneously.

We also performed calculations using double-folded (DF) real potentials to restrict the possible geometries to those expected from theoretical models. The optical potential used was of the form:

$$V(r)=N_{RC}V_C^{\mathrm{DF}}(r)+iW_C^{\mathrm{WS}}(r)+N_{LS}V_{LS}^{\mathrm{DF}}(r)\mathbf{l}\cdot\boldsymbol{\sigma}+V_{\mathrm{Coul}}\,, \tag{1}$$

where

$$W_C^{\mathrm{WS}}(r)=\frac{-W}{1+e^{(r-r_I)/a_I}}\,. \tag{2}$$

V_{Coul} is the usual Coulomb potential of a point projectile incident on a spherical charge distribution of radius $1.3A_T^{1/3}$, and the double-folded potentials V_{DF} were calculated as described by Eqs. (A3) and (A4) in the Appendix.

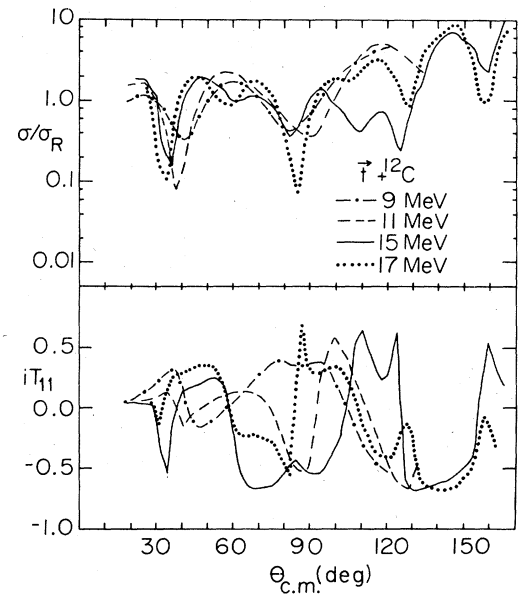

FIG. 2. Angular distributions of the differential cross section σ/σ_R (ratio-to-Rutherford) and of the vector analyzing powers iT_{11} for triton elastic scattering from ^{12}C at four energies, 9, 11, 15, and 17 MeV.

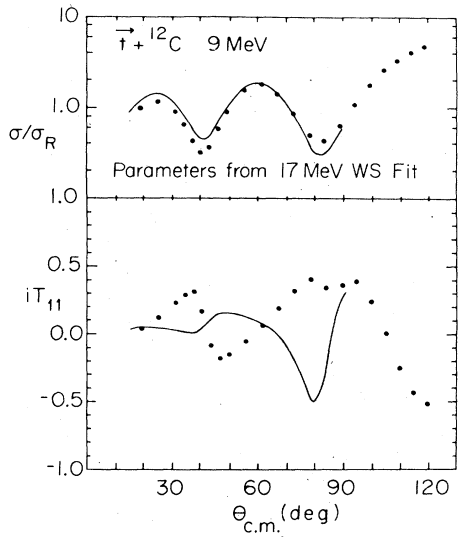

FIG. 3. Angular distribution of the differential cross section σ/σ_R (ratio-to-Rutherford) and of the vector analyzing power iT_{11} for 9 MeV triton elastic scattering from ^{12}C. The solid lines are the results of a fit to data taken at 17 MeV with Woods-Saxon shaped potentials.

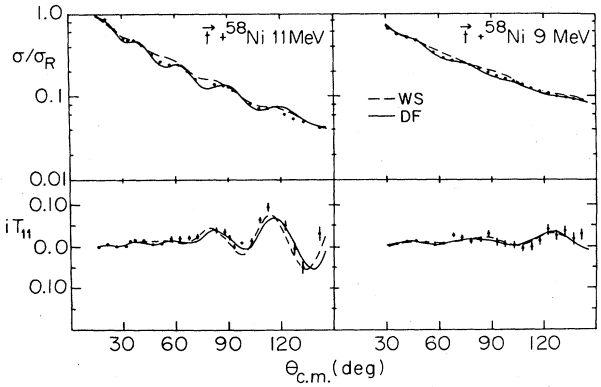

FIG. 4. Angular distributions of the differential cross section σ/σ_R (ratio-to-Rutherford) and of the vector analyzing powers iT_{11} for 9 and 11 MeV triton elastic scattering from ^{58}Ni. The solid lines display an optical model fit using double-folded central and spin orbit potentials. The dashed lines display a similar fit using Woods-Saxon potentials.

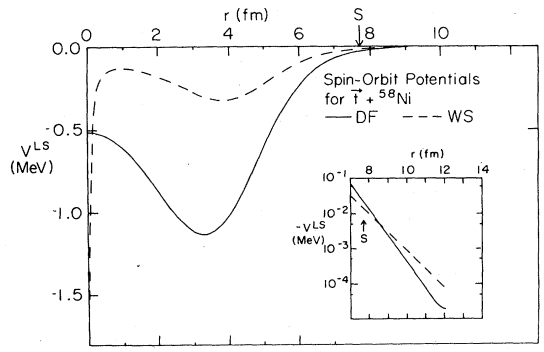

FIG. 5. Plot of spin-orbit potentials V_{LS} for the double-folded and Woods-Saxon cases $\vec{t}+{}^{58}$Ni. The arrow labeled S is the location of the strong absorption radius.

Microscopic double-folded potentials have been shown to give a good description of scattering for projectiles with $A<10$ if the real potential normalization N_{RC} is allowed to vary about 1.[8] There is less experience with the use of microscopic spin-orbit potentials, but values of $N_{LS}\sim 1$ have been successful in some studies.[9–11] In previous triton works, surface imaginary terms were used,[4,7] but we found that a volume shaped absorptive term gave an equally good fit. Calculations were performed using the optical model searching program HERMES (Ref. 12) which permits a search on N_{RC}, N_{LS}, W, r_I, and a_I if desired. The measured analyzing powers were converted to spherical notation for use in HERMES by dividing by $\sqrt{2}$, and, as in the Woods-Saxon case, only the data out to 90° c.m. were used in the fits because coupled-channels and resonant effects are traditionally thought to be important only at large angles.

We first investigated the use of double-folded potentials in a system for which isolated resonant effects should be small. Cross section and analyzing power data[4] for $\vec{t}+{}^{58}$Ni at 9 and 11 MeV were studied. Figure 4 displays our results along with the previously published fit using Woods-Saxon parameters. As can easily be seen, the double-folded potentials do an equally good job of fitting the data despite having fewer free parameters. More importantly, the data at both energies were reproduced by a common double-folded potential. This gives us some confidence that an energy independent microscopic potential is capable of describing triton elastic scattering in this energy regime. The resulting optical model parameters are listed in Table I. We do not know if any significance should be attributed to the need to use $N_{LS}\sim 3$ in the fit, since entrance channel effects are possible in this nucleus as well.[5] Figure 5 displays the spin-orbit potential V_{LS} for the double-folded and Woods-Saxon cases. It is only in the tail, beyond the strong absorption radius ($S\downarrow$) where the potentials are equal, that the scattering is presumed to take place.

The analysis of the $\vec{t}+{}^{12}$C scattering was based on the data at 9, 11, 15, and 17 MeV, shown in Fig. 2.[4,7] Our procedure was to first fit each individual energy. This produced four completely different parameter sets, just as in the Woods-Saxon case. However, none of the fits were able to reproduce the large forward angle oscillations in the analyzing powers. For each case, as the energy goes up, the oscillations in iT_{11} move to smaller angles but they never make it inside 60° for this energy range. This suggests that information about the spin-orbit potential is to be found by fitting mid to large angle data, $\theta>60°$. To confirm that the forward oscillations could not be fit, we searched on only the data with $\theta<60°$. While the cross sections were easily reproduced, no set of parameters was able to fit the forward oscillation in the analyzing powers. In each case, the backward angle analyzing power oscilla-

TABLE I. Optical model parameters for polarized triton scattering using double-folded real and spin-orbit potentials. The target densities used were:

$$^{58}\text{Ni: } \rho(r)=\frac{0.08152}{1+\exp\frac{(r-4.1156)}{0.55}}+\frac{0.08558}{1+\exp\frac{(r-4.1468)}{0.55}}\ \text{fm}^{-3}$$

$$^{12}\text{C: } \rho(r)=(0.173+0.0647r^2)e^{-(0.593r)^2}\ \text{fm}^{-3}$$

Target	E (MeV)	N_{RC}	N_{LS}	W (MeV)	r_I (fm)	a_I (fm)
^{58}Ni	9,11	1.05	3.45	27.1	1.63	0.45
^{12}C	9,11,15,17	1.15	3.45	16.04	1.92	0.52

tions were fit. Since double-folded potentials vary slowly with energy, we calculated cross sections and analyzing powers for each energy using the parameters from the 17 MeV fit. These parameters are also listed in Table I. In each case, the analyzing power was not reproduced by the calculation. However, all the cross sections were in rough agreement with the prediction based on the 17 MeV parameter set. Figure 6 displays the cross sections with a calculation using the tabulated parameters.

It seems that a simple double-folded central and spin-orbit potential model will not produce large analyzing powers at forward angles for this system in this energy range. This implies that the microscopic potentials are much more restrictive than the Woods-Saxon parametrization. The fact that the cross sections are fit but the analyzing powers are not suggests that the double-folding model reproduces the general trend of the data displayed in the cross sections while the analyzing powers are sensitive to more complicated interference effects. In the phenomenological Woods-Saxon analysis,[4] these effects were mocked up by drastic changes in the parameter sets.

We conclude from the present analysis that reliable information about the cluster-core spin-orbit potential cannot be obtained from presently available $\vec{t}+{}^{12}C$ data. The ${}^{12}C({}^{7}Li,\alpha)$ transfer reaction results suggest that entrance channel effects may be important in the energy region of the existing $\vec{t}+{}^{12}C$ data. This is supported by the large energy dependence in fitted phenomenological optical parameters which result as the many degrees of freedom in the form used[4] for this potential try to mock up the coupling to resonances in the entrance channel. The inability of the microscopic spin-orbit optical potentials to reproduce the forward angle analyzing power data results from geometric constraints in this model which limit the possible compensation for the failure to include the channel coupling. It is also possible that coupled-channels effects involving the ${}^{12}C$ 4.43 MeV state are important. Analyses of polarized ${}^{7}Li$ data[11] have shown that coupled-channels effects greatly influence the vector analyzing powers. These coupled-channels possibilities are best investigated by acquiring data for $\vec{t}+{}^{12}C$ scattering that fill in the excitation function, as emphasized by Slobodrian.[5] This would permit a quantitative analysis similar to that used in the detailed study of $\vec{p}+{}^{54}Fe$, where the energy dependence of phase shifts extracted from the data indicated the importance of coupling to the giant dipole resonance.[13] These data should include inelastic cross sections and analyzing powers to better define other possible coupled-channels effects that could be important in a calculation that treats each channel explicitly. A thorough analysis of more complete experimental information might permit the extraction of information about the strength of the cluster-core spin-orbit interaction which is necessary for structure calculations.

This work was supported in part by the National Science Foundation and the state of Florida.

APPENDIX

Because the triton is a spin-$\frac{1}{2}$ isospin-$\frac{1}{2}$ object, the double-folded potentials reduce to a form identical to local descriptions of nucleon-nucleus scattering[14] provided it is assumed that the projectile nucleons are all in $1s_{1/2}$ orbits and a factorization approximation is used to treat the knockout exchange amplitudes. For completeness, we outline the relevant results below using the notation of Ref. 10.

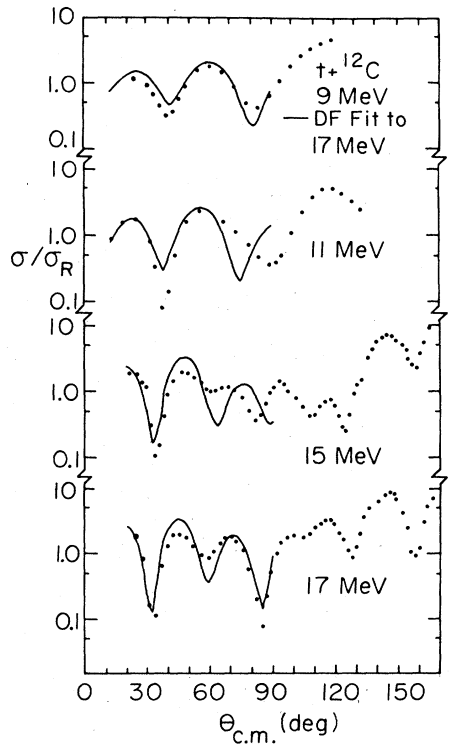

FIG. 6. Angular distributions of the differential cross sections for $\vec{t}+{}^{12}C$ at the four energies 9, 11, 15, and 17 MeV. The curves are calculations using a parameter set derived from fitting the 17 MeV data using double-folded central and spin-orbit potentials.

For this elastic scattering problem, it is sufficient to restrict consideration to the central spin-independent and spin-orbit components of a local, effective two-body interaction

$$v_{pt}(s)=\sum_T [g_{0T}^C(s)+g_T^{LS}(s)\mathbf{L}_{pt}\cdot\mathbf{S}_{pt}]\tau_p^T\cdot\tau_t^T \tag{A1}$$

such as that given by Bertsch *et al.*,[15] where

$$\mathbf{L}_{pt}\cdot\mathbf{S}_{pt}=\tfrac{1}{2}(\mathbf{s}\times\mathbf{p}_s)\cdot(\boldsymbol{\sigma}_p+\boldsymbol{\sigma}_t) \tag{A2}$$

is the usual spin-orbit operator, $\tau_i^0=1$ and $\tau_i^1=\tau_i$. The relevant optical potentials in Eq. (1) can be constructed directly from Eqs. (32), (33a), (31a), (33b), and (31b) of Ref. 10. These potentials are

$$V_C^{\mathrm{DF}}(r)=\sum_n w_n^2 j_0(k_n r)\sum_T [\tilde{g}_{0T}^C(k_n)\rho_T^{m,p}(k_n)\rho_T^{m,t}(k_n) + \tfrac{1}{2}\tilde{g}_T^{LS}(k_n)\rho_T^{m,p}(k_n)\rho_T^{ls,t}(k_n)] \tag{A3}$$

and

$$V_{LS}^{DF}(r)=(2)^{-1/2}(1/r)\frac{\partial}{\partial r}\times\sum_n w_n^2 j_0(k_n r)k_n^{-2}\times\sum_T[\tfrac{1}{2}\alpha\tilde{g}_T^{LS}(k_n)\rho_T^{s\perp,p}(k_n)\rho_T^{m,t}(k_n)]\ , \tag{A4}$$

where $\alpha=(3+A)/3A\simeq\frac{1}{3}$. The projectile matter (m) and dipole ($s\perp$) densities used are given by

$$\rho_T^{m,p}(q)=(4\pi)^{-1/2}\epsilon_{0T}e^{-a^2q^2/4}\ , \tag{A5}$$

$$\rho_T^{s\perp,p}(q)=(2\pi)^{-1/2}\epsilon_{1T}e^{-a^2q^2/4}\ , \tag{A6}$$

with $a=1.31$ fm and $\epsilon_{00}=3$, $\epsilon_{01}=\epsilon_{10}=1$, and $\epsilon_{11}=-1$ as in Ref. 14. The form of the spin-orbit potential in Eq. (A4) is identical to that used by Petrovich *et al.*[9]

The target matter densities used were defined by

$$\rho_T^{m,t}(q)=\int_0^\infty j_0(qr)\rho_T^{m,t}(r)r^2dr\ , \tag{A7}$$

where $\rho(r)$ is given in Table I. The normalization of ρ was chosen so that

$$\rho_T^{m,t}(0)=\begin{cases}A(4\pi)^{-1/2} & \text{for } T=0,\\ (N-Z)(4\pi)^{-1/2} & \text{for } T=1\ .\end{cases} \tag{A8}$$

It must be noted that the calculations described above assumed that $\rho_T^{ls,t}=0$ when calculating V_C^{DF}. This factor does not make a significant contribution to the central potential.

The interactions that appear in Eqs. (A3) and (A4) are given by

$$\tilde{g}_{0T}^{C}(q)=g_{0T}^{C,D}(q)+g_{0T}^{C,E}(Q)\ , \tag{A9}$$

$$\tilde{g}_T^{LS}(q)=g_T^{LS,D}(q)-(q^2/Q^2)g_T^{LS,E}(Q)\ , \tag{A10}$$

where

$$g_{0T}^{C}(q)=4\pi\int_0^\infty j_0(qs)g_{0T}^{C}(s)s^2ds\ , \tag{A11}$$

$$g_T^{LS}(q)=-4\pi q\int_0^\infty j_1(qs)g_T^{LS}(s)s^3ds\ , \tag{A12}$$

and $Q\cong\alpha\,|\,\mathbf{K}_i\,|$, where $\mathbf{K}_i$ is the initial wave number of the projectile. The superscripts D and E refer to direct and exchange, with the g^E constructed by reversing the signs of the odd (even) state components in g^D for the central (spin-orbit) interaction. Because $g^{LS}(s)$ is short range, the $\tilde{g}_T^{LS}(q)$ used here are almost identical to the commonly used[9,10] approximation $2g_T^{LS,\text{odd}}(q)$, where g^{odd} is constructed from the odd state spin-orbit interaction alone.

The double-folded potentials were generated by a modified version of the code ALLWRLD (Ref. 16) that was previously used for the calculations of Refs. 14 and 17. These were then read into HERMES,[12] which solved the elastic scattering equations.

[1]H. G. Bingham, H. T. Fortune, J. D. Garrett, and R. Middleton, Phys. Rev. Lett. **26**, 1448 (1971); D. K. Scott, P. N. Hudson, P. S. Fisher, C. U. Cardinal, N. Aryas-Weiss, A. D. Panagioton, P. J. Ellis, and B. Buck, *ibid.* **28**, 2659 (1972); K. Nagatani, D. H. Youngblood, R. Kenefick, and J. Bronson, *ibid.* **31**, 250 (1973); H. G. Bingham, M. L. Halbert, D. C. Hensley, E. Newman, K. W. Kemper, and L.A. Charlton, Phys. Rev. C **11**, 1913 (1975).

[2]B. Buck, C. B. Dover, and J. P. Vary, Phys. Rev. C **11**, 1803 (1975); B. Buck and A. A. Pilt, Nucl. Phys. **A280**, 133 (1977); B. Buck, H. Friedrich, and A. A. Pilt, *ibid.* **A290**, 205 (1977); B. Buck and A. A. Pilt, *ibid.* **A295**, 1 (1978); A. A. Pilt, Nuovo Cimento **74A**, 185 (1983).

[3]A. C. Merchant, Phys. Lett. **130B**, 241 (1983); J. Phys. G **9**, 1169 (1983); **10**, 273 (1984).

[4]D. Fick, R. E. Brown, W. Grüebler, R. A. Hardekopf, and J. S. Hanspal, Phys. Rev. C **29**, 324 (1984).

[5]R. J. Slobodrian, Phys. Rev. C **29**, 2353 (1984).

[6]A. F. Zeller, K. W. Kemper, T. R. Ophel, and A. Johnston, Nucl. Phys. **A344**, 307 (1980).

[7]P. A. Schmelzbach, R. A. Hardekopf, R. F. Haglund, Jr., and G. G. Ohlsen, Phys. Rev. C **17**, 16 (1978).

[8]G. R. Satchler and W. G. Love, Phys. Rep. **55**, 183 (1979).

[9]F. Petrovich, D. Stanley, L. A. Parks, and P. Nagel, Phys. Rev. C **17**, 1642 (1978).

[10]F. Petrovich, R. J. Philpott, A. W. Carpenter, and J. A. Carr, Nucl. Phys. **A425**, 609 (1984).

[11]G. Tungate, R. Bottger, P. Egelhof, K.-H. Mobius, Z. Moroz, E. Steffens, W. Dreves, I. Koenig, and D. Fick, Phys. Lett. **98B**, 347 (1981); H. Nishioka, R. C. Johnson, J. A. Tostevin, and K. I. Kubo, Nucl. Phys. **A415**, 230 (1984); H. Ohnishi, M. Tanifuji, M. Kamimura, Y. Sakuragi, and M. Yahiro, *ibid.* **A415**, 271 (1984); D. Mukhopadhyay, G. Grawert, D. Fick, and Z. Moroz, Phys. Lett. **104B**, 361 (1981).

[12]J. Cook, Comput. Phys. Commun. **31**, 363 (1984).

[13]H. R. Weller, J. Szucs, J. A. Kuehner, G. D. Jones, and D. T. Petty, Phys. Rev. C **13**, 1055 (1976).

[14]S. L. Tabor, G. Neuschaefer, J. A. Carr, F. Petrovich, C. C. Chang, A. Guterman, M. T. Collins, D. L. Friesel, C. Glover, S. Y. Van Der Werf, and S. Raman, Nucl. Phys. **A422**, 12 (1984).

[15]G. Bertsch, J. Borysowicz, H. McManus, and W. G. Love, Nucl. Phys. **A284**, 399 (1977).

[16]J. A. Carr, F. Petrovich, D. Halderson, and J. Kelly, Computer program ALLWRLD (unpublished).

[17]C. Ellegaard, C. Gaarde, J. S. Larsen, C. Goodman, I. Bergqvist, L. Carlen, P. Ekstrom, B. Jakobsson, J. Lyttkens, M. Bedjidian, M. Chamcham, J. Y. Grossiord, A. Guichard, M. Gusakow, R. Haroutunian, J. R. Pizzi, D. Bachelier, J. L. Boyard, T. Hennino, J. C. Jourdain, M. Roy-Stephan, M. Boivin, and P. Radvanyi, Phys. Rev. Lett. **50**, 1745 (1983).